INSTITUTO POLITÉCNICO DE BRAGANÇA
Escola Superior de Tecnologia e Gestão

Drag coefficients in hydraulic channel

Mohamed Chiheb AOUSSAJI

Work performed under the supervision of

Prof. Dr. Sérgio Rosa

Master in Mechanical Engineering

2023-2024

Drag coefficients in hydraulic channel

Master in Mechanical Engineering

Escola Superior de Tecnologia e Gestão

Instituto Politécnico de Bragança

Mohamed Chiheb AOUSSAJI

2023-2024

Dedication

To my dearest Parents, I can never express the gratitude, pride and deep love I have for the sacrifices you have made for my success. Your prayers, encouragement and support have always been a great help to me.

To my dear brothers, for their love and affection. May God bless you and keep you in his peace

To my dear friends, your precious collaboration and friendly support have been a source of inspiration and encouragement to me. May God give you happiness and prosperity.

To all the people who, actively or not, participated and helped in the accomplishment of this work.

To all those who I love, I dedicate this work

Acknowledgements

First of all, I would like to thank Allah, the Almighty and the Merciful, who has given me the strength and patience to accomplish this humble work.

With the most sincere gratitude, I would like to thank my supervisors ***Prof. Dr. Sérgio Rosa***, for all the effort, the constant help and the trust, without his active participation and encouragement this work would not have been done. You have been an undeniable source of motivation and working with you has been a real pleasure. I would like to express my deepest gratitude to the members of the scientific committee for their kindness in reading this study and their interest in reviewing this document and enriching it with their proposals.

Finally, may all the people, who contributed to the accomplishment of this project, find here the expression of my respectful gratitude and the testimony of my dedication...

Abstract

For effective modeling and prediction of body behaviors on external fluid flows, in order to improve design and performance, it is crucial to comprehend the drag forces. The geometry of the body, the Reynolds number, and the roughness surface of the body, are some of the variables that affect the drag force. As a result, the availability of a water tunnel channel is an essential tool for conducting experimental testing in a way that is quick and affordable while incorporating all of the complexity of a real flow, allowing for the quantification of drag forces, or the overall resistance of a body being dragged by a fluid.

Keywords: External flows,drag coefficient, water tunnel, bodies geometry.

Resumo

Para a modelação eficaz e previsão do comportamento de corpos em escoamentos exteriores„ por forma a melhorar o design e o desempenho, é crucial compreender as forças de arrasto. A geometria do corpo, o número de Reynolds e a rugosidade da superfície da superfície do corpo, são algumas das variáveis que afetam o valor do coeficiente de arrastamento. Como resultado, a disponibilidade de um canal de túnel de água é uma ferramenta essencial para a realização de testes experimentais em um forma que é rápida e acessível enquanto incorporando toda a complexidade de um fluxo real, permitindo a quantificação das forças de atrito, ou a resistência geral de um corpo ser arrastado por um fluido.

Palavras-chave: Excoamentos exteriores, coeficiente de arrasto, túnel de água, geometria de corpos.

Contents

List of Tables

List of Figures

Acronyms

μ Dynamic viscosity.

ν Kinematic viscosity.

ρ Density.

τ Tangential force.

A Projected cross-sectional area.

CD Drag Coefficient.

FD Drag Force.

Re Reynold number.

V Velocity.

Chapter 1

Introduction

1.1 Context

Fluid dynamics, particularly in the context of external flows, plays a crucial role in various engineering and scientific applications. External flows refer to the motion of a fluid around a body immersed in it, such as air flowing around an aircraft or water flowing around a ship's hull. Understanding external flows is essential for predicting the behavior of objects, structures, and other objects in fluid environments.

One of the key aspects of external flows is the concept of drag force. Drag force is the resistance experienced by a body moving through a fluid, and it is caused by the interaction between the body and the fluid. This force can be divided into two main components: pressure drag, which is due to the pressure distribution around the body, and skin drag friction, which is caused by the viscosity of the fluid. The drag force is an important consideration in the design of vehicles and structures, as it affects their performance and energy efficiency.

The drag coefficient is a dimensionless quantity that is used to quantify the drag or resistance of an object in a fluid environment. It is a key parameter in aerodynamics and fluid dynamics, and it is influenced by the shape of the body and the properties of the fluid. A lower drag coefficient indicates that the object will have lower aerodynamic drag

force, leading to higher energy efficiency.

Aerodynamics, which is a subfield of fluid dynamics, focuses on the study of the motion of air and other gases, particularly in relation to the movement of objects through the air. It is a fundamental aspect of understanding external flows, as it provides insights into the behavior of vehicles, aircraft, and other objects in fluid environments.

In summary, fluid dynamics, especially in the context of external flows, is essential for understanding the behavior of objects in fluid environments, predicting drag forces, and optimizing the design and performance of various engineering systems. It encompasses concepts such as drag force, drag coefficient, and aerodynamics, which are fundamental to the study of fluid motion and its practical applications.

1.2 Objectives

The primary goal of this study is to experimentally determine the necessary drag forces for various object shapes. This investigation maintains a consistent velocity of the fluid throughout multiple experiments conducted in a hydraulic channel. By conducting these experiments it was possible to gain insights into how different shapes affect the drag force and also how the viscosity of the fluid interact with the drag force, and so contributing to a deeper understanding of drag forces and their dependence on fluid viscosity. For the purpose of validation, well-established and documented geometries with known drag coefficients from existing literature will be employed.

1.3 Document structure

This study is structured into distinct chapters, each contributing to a comprehensive exploration of the subject matter. The organization of this report is as follows:

Chapter 1: Introduction

The fundamental principles of fluid mechanics are elucidated in this chapter, offering an extensive insight into the dynamics of internal and external flows.

Chapter 2: Theoretical Foundation and Fluid Mechanics

In this chapter, fundamental principles of fluid mechanics are elucidated, offering insight into the dynamics of flows and forces. Additionally, it delves into the utilization of a water tunnel as a pivotal research tool.

Chapter 3: Methodology and Experimental Setup

Detailed methodology employed in conducting experimental activities is elaborated in this chapter. It encompasses the procedural steps, accompanied by relevant images, and considerations pertaining to both test models and flow conditions.

Chapter 4: Results and Analysis

Chapter 4 unveils the outcomes derived from experimental tests. These results are subjected to meticulous qualitative and, wherever feasible, quantitative validation and discussion.

Chapter 5: Conclusions and Future Directions

The final chapter encapsulates the broader conclusions drawn from the study's analysis of results, identifying key limitations. Furthermore, this section offers a succinct overview of potential avenues for future research.

Chapter 2

Literature review

This chapter introduces fundamental fluid mechanics principles and explores the fluid dynamics of internal and external flows. Furthermore, the chapter provides an insight into published results, showcasing real applications of fluid mechanics and its significance in external flow scenarios. In summary, this chapter bridges theory and practice, offering a foundational understanding of fluid mechanics while highlighting its practical implications.

2.1 Fluid Properties

A fluid is a material that undergoes continual deformation when subjected to even the slightest amount of shear stress. Alternatively, a fluid may be defined as a material that is incapable of maintaining a shear stress when in a state of rest.[1]

2.1.1 Viscosity

Viscosity is the most important property of liquid which measures the resistance of the fluid to shear stress or shear rate. When a fluid layers move relative to one other, intermolecular friction causes shear resistance, so the viscosity can be understood as the measure of a fluid's resistance to flow or its resistance to deformation. The absolute

or Dynamic viscosity (μ) is the amount of Tangential force (τ) per unit area needed to move one horizontal plane relative to another while maintaining a unit velocity and unit distance in the fluid.[2]

$$\begin{aligned} \tau &= \mu dc/dy \\ &= \mu\gamma \end{aligned} \tag{2.1}$$

Equation (2.1) is known as the Newtons Law of Friction. (2.1) can be rearranged to express Dynamic viscosity as

$$\begin{aligned} \mu &= \tau dy/dc \\ &= \tau/\gamma \end{aligned} \tag{2.2}$$

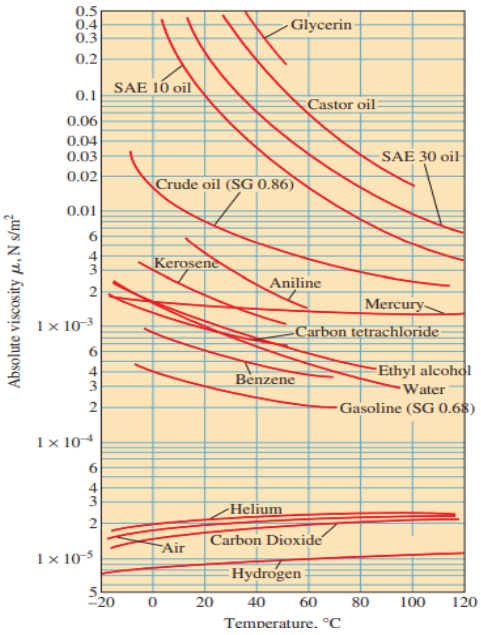

Figure 2.1: dynamic (absolute) viscosity of common fluids

Kinematic viscosity (ν) is defined as the quotient of absolute viscosity (also known as dynamic viscosity) divided by density. It is a measure that does not entail any force. Kinematic viscosity is determined by dividing the absolute viscosity of a fluid by the fluid's mass density.[2]

$$v = \mu/\rho \tag{2.3}$$

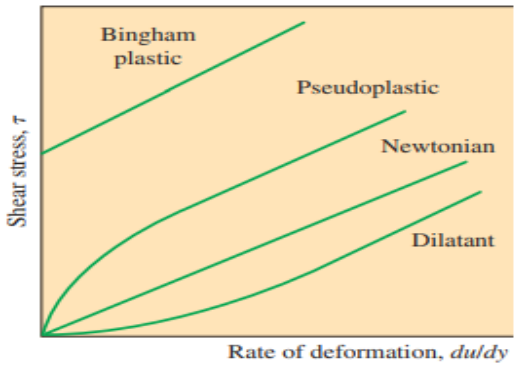

Figure 2.2: Variation of shear stress with the rate of deformation for Newtonian and non-Newtonian fluids

In the case of non-Newtonian fluids, the connection between shear stress and rate of deformation is not linear. The gradient of the curve on the τ vs du/dy graph is known as the apparent viscosity of the fluid. Fluids that experience an increase in apparent viscosity as the rate of deformation rises, such as solutions containing suspended starch or sand, are known as dilatant or shear thickening fluids. On the other hand, fluids that display the opposite behavior, becoming less viscous as they are subjected to higher shear forces, like certain paints, polymer solutions, and fluids with suspended particles, are referred to as pseudoplastic or shear thinning fluids. Certain substances, like toothpaste, have the ability to withstand a limited amount of shear stress and hence exhibit solid-like behavior. However, when the shear stress surpasses the yield stress, these substances undergo continuous deformation and exhibit fluid-like behavior. The materials in question are often known as Bingham plastics.

Typically, the viscosity of a fluid is influenced by both temperature and pressure, but the impact of pressure is quite insignificant. Regarding liquids, both the dynamic and kinematic viscosities are mostly unaffected by pressure, and any minor changes in pressure are often ignored, especially under extremely high pressure conditions. Regarding gases, this principle applies to dynamic viscosity at low to moderate pressures, but not to kinematic viscosity due to the direct relationship between gas density and pressure.[3]

2.1.2 Density

Density is a ubiquitous and significant characteristic of matter. Density, in the context of a liquid, refers to the amount of mass present inside a given volume. Volumetric mass density is the most accurate term for density. Density (ρ) is a mathematical concept that represents the ratio of the mass (m) to the volume (V) of a material or body:

$$\rho = \frac{m}{V}$$

The unit of measurement for density in Sl is $\mathbf{kg/m^3}$. Liquids undergo volumetric thermal expansion, wherein their volume rises with an increase in temperature.

Hence, the density of a certain liquid is not consistent when there are fluctuations in temperature. The density function of temperature is dependent on:

$$\rho = \frac{\rho_{T0}}{1 + \alpha \cdot \Delta T}$$

$\rho_{TO}\left[\text{ kg/m}^3\right]$-density at a reference temperature T_0

$\alpha\,[1°\text{C}]$-thermal expansion coefficient of the liquid at temperature T_0

$\Delta T\,[°\text{C}]$ - temperature difference

$\Delta T = T - T_0$

density of some substance.[4]

Substance	**Phase**	**Density[kg/m^3]**
Water	liquid	1000
Rubbing alcohol	liquid	786
Aluminium	solid	2700
Wax	solid	930

Table 2.1: Fluid density

2.2 Internal flow

Fluid flow is categorized as either internal or external, based on whether the fluid moves within a limited area or over a surface.[3]

An internal flow refers to the movement of fluid inside a pipe, duct, or channel that has walls or a free surface to direct the flow from an intake point to an output point, without any specific restrictions on the initial and final states of the flow.

Laminar flow, also known as Poiseuille flow, occurs when fluid moves smoothly through a circular pipe. This is considered the simplest kind of internal flow. On the other hand,

turbulent flow, which occurs in the impeller and diffuser of a centrifugal compressor stage, is one of the most complicated forms of internal flow.

As per this definition, the flow over a model in a wind tunnel is considered a "internal flow". However, the key difference between external flows and internal flows is that in the latter, the shear layers on the walls interact significantly with each other or, at the very least, with the "inviscid" fluid between them. We include certain phenomena that may also manifest in external flows due to their higher prevalence, broader applicability, or greater ease of discussion in the context of internal flows. Poiseuille flow and its turbulent counterpart are considered to be completely developed, which means that the flow field remains constant, in terms of ensemble or time-mean, regardless of the location along the duct in the streamwise direction. Internal flows are the only kind of flows that exhibit fully developed flow. It is by definition a flow type that is independent of inlet or outlet state and one where conditions are statistically identical at each axial position. Turbulence researchers frequently prefer fully developed duct flows due to their simplicity. Practically, many internal flows are not completely formed, however they may include wall boundary layers, slender inner shear layers (wakes or jets), and extensive areas of almost inviscid flow.[5]

2.3 External flow

External flow refers to the movement of an unbounded fluid across a surface, such as a plate, wire, or pipe. airflow over a ball or an exposed pipe on a windy day is categorized as external flow. Open-channel flow refers to the movement of liquids in a partially filled duct with a free surface. The movement of water in rivers and irrigation canals exemplify such fluid dynamics. The effect of viscosity is the main factor in determining the behavior of internal flows over the whole flow field. Viscous effects in external flows are confined to boundary layers adjacent to solid surfaces and to wake regions located downstream of bodies.[3]

2.3.1 Reynolds Number and Flow Regimes

The Reynold number (Re) is a dimensionless parameter utilized to predict the nature of fluid flow in a certain scenario. Fluid mechanics engineers rely on this technology to forecast flow patterns and enhance later designs by modifying or optimizing them for improved flow.[6]

The fact of the matter is that no general analysis of fluid motion yet exists. There are several dozen known particular solutions, there are many approximate digital computer solutions, and there are a great many experimental data. There is a lot of theory available if we neglect such important effects as viscosity and compressibility, but there is no general theory and there may never be. The reason is that a profound and vexing change in fluid behavior occurs at moderate Reynolds numbers.[7] the primary parameter correlating the viscous behavior of all newtonian fluids is the dimensionless Reynolds number:

$$Re = \frac{\rho V L}{\mu} = \frac{V L}{v} \tag{2.4}$$

where V and L are characteristic velocity and length scales of the flow. The second form

of Re illustrates that the ratio of μ to ρ has its own name, the kinematic viscosity:

$$\nu = \frac{\mu}{\rho} \tag{2.5}$$

kinematic viscosity has units m^2/s, and can be viewed as viscous diffusivity or diffusivity for momentum.[3]

Reynolds Number in Internal Flow

Generally, the first thing a fluids engineer should do is estimate the Reynolds number range of the flow under study. Very low Re indicates viscous creeping motion, where inertia effects are negligible. Moderate Re implies a smoothly varying laminar[7] flow which is less common in practice and is characterized by the highly ordered movement of fluid layers, such as highly viscous fluids such as oils flowing at low speeds[8]. High Re probably spells turbulent flow, which is slowly varying in the time-mean but has superimposed strong random high-frequency fluctuations. Explicit numerical[7] which is more common in everyday engineering applications, is observed for randomness and high velocity fluctuations, as occurs in the flow of low viscosity fluids such as air, at high speeds[8]

Under most practical conditions, the flow in a circular pipe is laminar for Re $\lesssim$ 2300, turbulent for Re $\gtrsim$ 4000, and transitional in between. That is,

- Re $\lesssim$ 2300 laminar flow
- 2300 $\lesssim$ Re $\lesssim$ 4000 transitional flow
- Re $\gtrsim$ 4000 turbulent flow

In transitional flow, the flow switches between laminar and turbulent in a disorderly fashion. It should be kept in mind that laminar flow can be maintained at much higher Reynolds numbers in very smooth pipes by avoiding flow disturbances and pipe vibrations. In such carefully controlled laboratory experiments, laminar flow has been maintained at Reynolds numbers of up to 100,000.[3]

Reynolds Number in External Flow

The external flow, in which the mainstream does not have clear boundaries, is similar to internal flow, which also exhibits a transition regime. The effect of velocity throughout the stream is commonly studied by examining flows over bodies such as a flat plate, cylinder, and sphere, which serve as standard cases. In 1914, German scientist Ludwig Prandtl made the discovery of the boundary layer, which is influenced by the Reynolds number and encompasses the surface in different states of flow, including laminar, turbulent, and transitional regimes. The diagram illustrates the flow over a flat surface, depicting different regimes. In this context, x_c represents the critical length for transition, L denotes the total length of the plate, and u represents the velocity of the free streamflow.

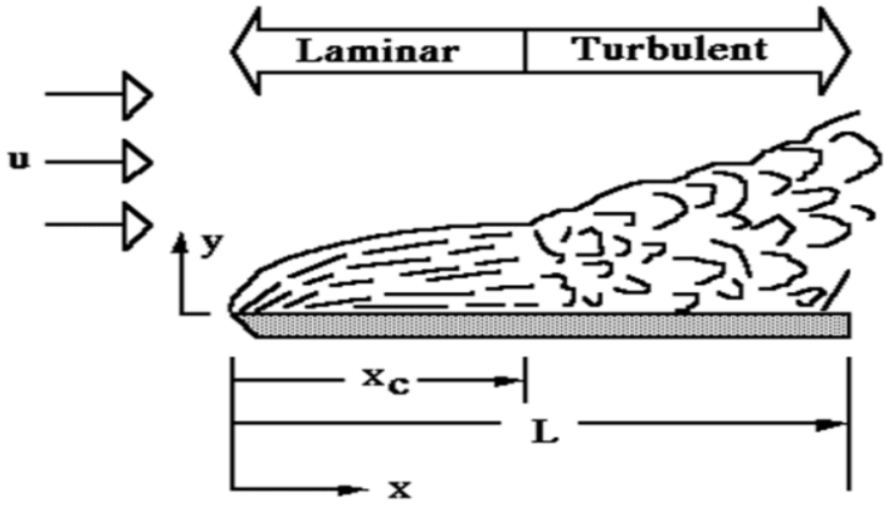

Figure 2.3: Transition of the boundary layer for flow over the flat plate surface with critical length for transition regime.

Typically, the boundary layer expands as it moves along the x direction on the plate, leading to unstable conditions where the Reynolds number also increases. The critical Reynolds number for flow over a flat plate surface is:

$$Re_{\text{critical}} = \frac{\rho V x}{\mu} \geq 3 \times 10^5 \text{ to } 3 \times 10^6 \tag{2.6}$$

which is contingent upon the consistency of the flow across the surface. Although the

critical Reynolds numbers for internal flow regimes are well-defined, it is challenging to determine them for external flow due to the variation in critical Reynolds numbers based on geometry. In addition, in the case of external flow, boundary layer separation poses a unique challenge, as there are various uncertainties involved in creating a dependable numerical model within a specific physical area.[9]

Flow regime

In contrast, the Reynolds number plays a crucial role in understanding compressible and incompressible flow regime. A flow is classified as being compressible or incompressible, depending on the level of variation of density during flow. Incompressibility is an approximation, in which the flow is said to be incompressible if the density remains nearly constant throughout. Therefore, the volume of every portion of fluid remains unchanged over the course of its motion when the flow is approximated as incompressible. The densities of liquids are essentially constant, and thus the flow of liquids is typically incompressible. Therefore, liquids are usually referred to as incompressible substances. A pressure of 210 atm, for example, causes the density of liquid water at 1 atm to change by just 1 percent. Gases, on the other hand, are highly compressible. A pressure change of just 0.01 atm, for example, causes a change of 1 percent in the density of atmospheric air. the flow speed is often expressed in terms of the dimensionless Mach number defined as

$$\text{Ma} = \frac{V}{c} = \frac{\text{Speed of flow}}{\text{Speed of sound}} \tag{2.7}$$

where c is the speed of sound whose value is 346 m/s in air at room temperature at sea level. A flow is called sonic when Ma = 1, subsonic when Ma $<$ 1, supersonic when Ma $>$ 1, and hypersonic when Ma $\gg$ 1. Liquid flows are incompressible to a high level of accuracy, but the level of variation of density in gas flows and the consequent level of approximation made when modeling gas flows as incompressible depends on the Mach number. Gas flows can often be approximated as incompressible if the density changes are under about 5 percent, which is usually the case when Ma , 0.3. Therefore, the

compressibility effects of air at room temperature can be neglected at speeds under about 100 m/s. Small density changes of liquids corresponding to large pressure changes can still have important consequences. The irritating "water hammer" in a water pipe, for example, is caused by the vibrations of the pipe generated by the reflection of pressure waves following the sudden closing of the valves.[3]

2.3.2 Boundary Layer Theory

Boundary layer theory is a fundamental concept in fluid dynamics that focuses on the thin layer of fluid adjacent to a solid surface. This layer, known as the boundary layer, is characterized by a gradual transition of fluid velocity from zero at the solid surface to the free stream velocity away from the surface. there are at least two flow situations in which the viscous term in the Navier–Stokes equation can be neglected. The first occurs in high Reynolds number regions of flow where net viscous forces are known to be negligible compared to inertial and pressure forces, we call these inviscid regions of flow. The second situation occurs when the vorticity is negligibly small, we call these irrotational or potential regions of flow. In either case, removal of the viscous terms from the Navier–Stokes equation yields the Euler equation are themselves approximations of the full Navier–Stokes equation

$$\rho \left[\frac{\partial \vec{V}}{\partial t} + (\vec{V} \cdot \vec{\nabla})\vec{V} \right] = -\vec{\nabla} P + \rho \vec{g} \tag{2.8}$$

While the math is greatly simplified by dropping the viscous terms, there are some serious deficiencies associated with application of the Euler equation to practical engineering flow problems. High on the list of deficiencies is the inability to specify the no-slip condition at solid walls. This leads to unphysical results such as zero viscous shear forces on solid walls and zero aerodynamic drag on bodies immersed in a free stream. We can therefore think of the Euler equation and the Navier–Stokes equation as two mountains separated by a huge chasm A major breakthrough in fluid mechanics occurred in 1904 when Ludwig Prandtl (1875–1953) introduced the boundary layer approximation. Prandtl's idea was to

divide the flow into two regions: an outer flow region that is inviscid and/or irrotational, and an inner flow region called a boundary layer—a very thin region of flow near a solid wall where viscous forces and rotationality cannot be ignored.

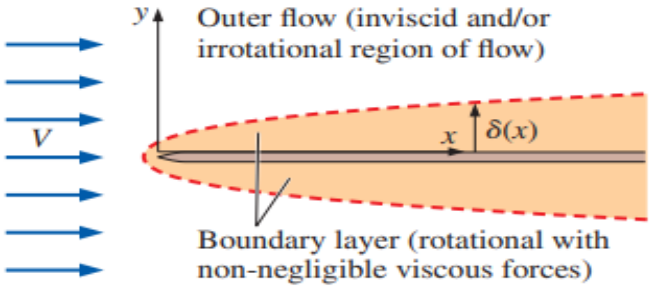

Figure 2.4: boundary layer concept

In the outer flow region, we use the continuity and Euler equations to obtain the outer flow velocity field, and the Bernoulli equation to obtain the pressure field. Alternatively, if the outer flow region is irrotational, we may use the potential flow techniques The key to successful application of the boundary layer approximation is the assumption that the boundary layer is very thin. The classic example is a uniform stream flowing parallel to a long flat plate aligned with the x-axis. Boundary layer thickness δ at some location x along the plate is sketched in Fig. (2-5). By convention, δ is usually defined as the distance away from the wall at which the velocity component parallel to the wall is 99 percent of the fluid speed outside the boundary layer. It turns out that for a given fluid and plate, the higher the free-stream speed V, the thinner the boundary layer (Fig. 2-4). In nondimensional terms, we define the Reynolds number based on distance x along the wall,

$$\text{Reynolds number along a flat plate:} \quad \text{Re}_x = \frac{\rho V x}{\mu} = \frac{V x}{\nu} \tag{2.9}$$

Hence, At a given x-location, the higher the Reynolds number, the thinner the boundary layer.

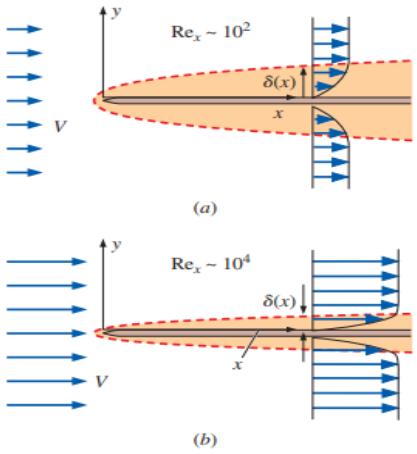

Figure 2.5: Flow of a uniform stream parallel to a flat plate

In real-life engineering flows, transition to turbulent flow usually occurs more abruptly and much earlier (at a lower value of Rex) than the values given for a smooth flat plate with a calm free stream. Factors such as roughness along the surface, free-stream disturbances, acoustic noise, flow unsteadiness, vibrations, and curvature of the wall contribute to an earlier transition location. Because of this, an engineering critical Reynolds number of $\mathrm{Re}_{x,\mathrm{cr}} = 5\times10^5$ is often used to determine whether a boundary layer is most likely laminar ($\mathrm{Re}_x < \mathrm{Re}_{x,\mathrm{cr}}$) or most likely turbulent ($\mathrm{Re}_x > \mathrm{Re}_{x,\mathrm{cr}}$). It is also common in heat transfer to use this value as the critical Re_x in fact, relations for average friction and heat transfer coefficients are derived by assuming the flow to be laminar for Rex lower than $\mathrm{Re}_{x,\mathrm{cr}}$, and turbulent otherwise. The logic here is to ignore transition by treating the first part of transition as laminar and the remaining part as turbulent

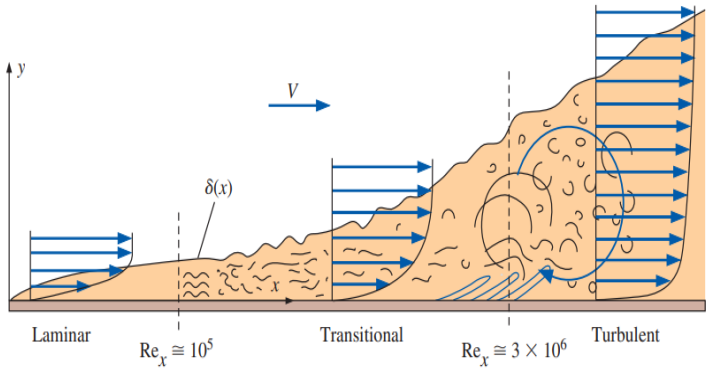

Figure 2.6: Transition of the laminar boundary layer on a flat plate into a fully turbulent boundary layer

The transition process is unsteady as well and is difficult to predict, even with modern CFD codes. In some cases, engineers install rough sandpaper or wires called trip wires along the surface, in order to force transition at a desired location . The eddies from the trip wire cause enhanced local mixing and create disturbances that very quickly lead to a turbulent boundary layer.[3]

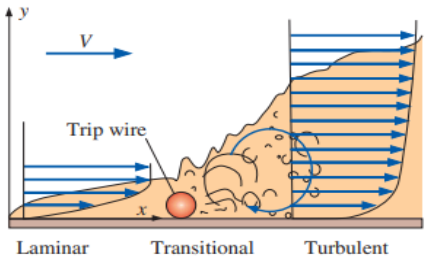

Figure 2.7: initiate early transition to turbulence in a boundary layer

2.3.3 Separation Phenomena

The flow behavior at relatively high Reynolds numbers around blunt bodies or through steeply expanding channels or conduits deviates significantly from the anticipated flow pattern based on inviscid theory. (Figure 2.8) illustrates two instances of these flow patterns, one using a sphere and the other including a duct or pipe with a downstream extension at a specific location. At the location where the solid boundary starts to deviate or move away from the direction of the average flow, the boundary layer detaches or splits from the boundary. The occurrence is referred as flow separation.

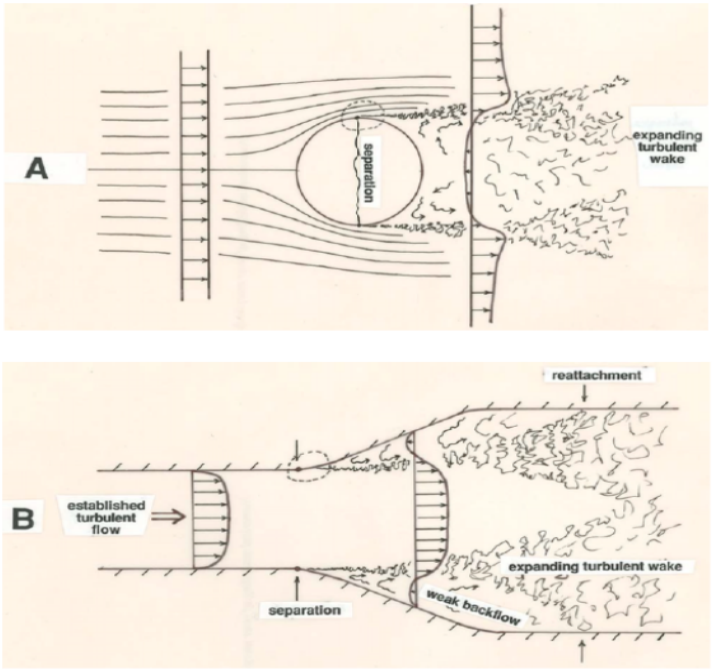

Figure 2.8: flow separation (A) around a sphere and (B) through an expansion in a planar duct

The flow always separates from the boundary so that the fluid continues straight ahead as the boundary surface falls away from the flow upstream. The main flow outside the boundary layer diverges from the solid boundary. In (Figure 2.8) the dashed curves indicate that flow separation is influenced by the orientation of the boundary relative to the overall flow, which involves a curving away from the overall flow direction. Separation occurs downstream of this curving away. The stagnant fluid downstream of the separation

point has about the same average velocity as the boundary. In this region the fluid has an unsteady eddying pattern of motion, with only a weak circulation as shown in (Figure 2.8). Once the boundary layer leaves the solid boundary, it contacts this slower-moving fluid across a strong shear surface. A short distance downstream of the separation point, this unstable shearing surface becomes wavy and breaks down to produce turbulence. This turbulence is mixed or diffused into the main flow and stagnant region, and viscous shearing in eddies dampens it, but its effect extends for a great distance downstream. Wakes are the stagnant fluid inside the separation surface and the strong turbulence on it. Long downstream from a blunt body like a sphere (Figure A 2.8), wake turbulence is weak and the average fluid velocity across the mean flow is slightly less than free-stream velocity. The expanding zone of wake turbulence eventually impinges on the boundary in flow past an expansion in a duct or channel (Figure B 2.8). Downstream of this point, the flow reattaches to the boundary, and a new boundary layer develops until the flow is fully established well downstream of the expansion.

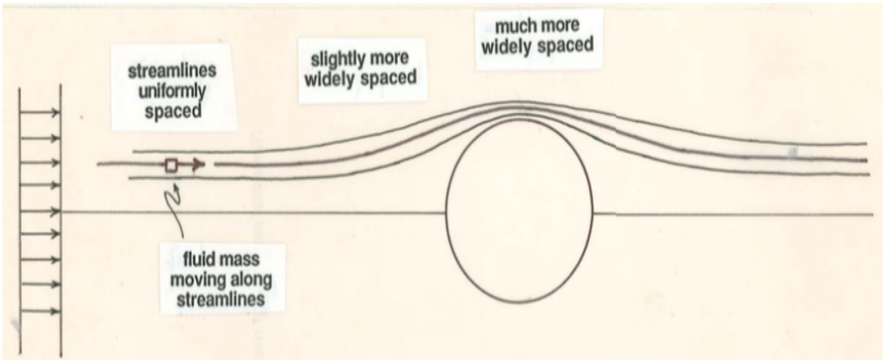

Figure 2.9: Pattern of streamlines in steady inviscid flow past a sphere.

Flow separation is explained by steady inviscid flow around a sphere (Figure 2.9). Remember that spacing between streamlines can qualitatively indicate fluid velocity. A small mass of fluid approaches the sphere along a streamline that will bring it close to the surface, decelerating slightly from its uniform velocity before accelerating to a maximum velocity at the midsection (Figure 2.10 A). Beyond the midsection, it decelerates to minimum velocity and then accelerates slightly to free-stream velocity. Applying the

Bernoulli equation

$$p_2 - p_1 = -\frac{\mu}{2}\left(v_2^2 - v_1^2\right) \tag{2.10}$$

to determine fluid pressure variation (Figure 2.10 B). The pressure is slightly higher than free-stream at the sphere's upstream and downstream extremities but lowest at the midsection. As the fluid passes around the sphere, pressure variation causes strong accelerations and decelerations. In front of the sphere, the pressure decreases along the streamline (the spatial rate of change or gradient of pressure is negative or favorable), Pressure rises along the streamline behind the sphere, creating a net force that slows the fluid mass.

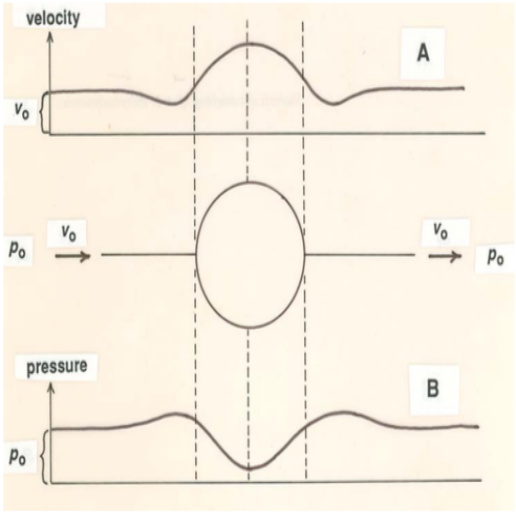

Figure 2.10: Variation in A) velocity and B) pressure along a streamline passing close to the surface of a sphere, for steady inviscid flow past the sphere

In inviscid flow the pressure is the only force in the fluid. But in the real world of viscous fluids, a boundary layer develops next to the sphere (Figure 2.11). If the boundary layer is thin, the streamwise variation in fluid pressure given by the Bernoulli equation along streamlines just outside the boundary layer is approximately the same as the pressure on the boundary. If now you follow the motion of a fluid mass along a streamline that is close enough to the sphere to become involved in the boundary layer, a viscous force as well as the impressed pressure force acts on the fluid mass. Because the viscous force everywhere opposes the motion, the fluid mass cannot ultimately regain its uniform velocity after passing the sphere, as in inviscid flow. The fluid cannot accelerate as much in front of the sphere as in inviscid flow, so it reaches the midsection with lower velocity. The adverse pressure gradient in back of the sphere, reinforced by viscous retardation, decelerates the fluid to zero velocity and causes it to reverse. The reverse flow blocks the front of the sphere's flow, thus it must break away from the border to pass over it. This slowdown to zero velocity happens just a short distance downstream of the unfavorable pressure gradient where the boundary bends away from the mean flow direction because streamlines near the boundary have low velocities.[10]

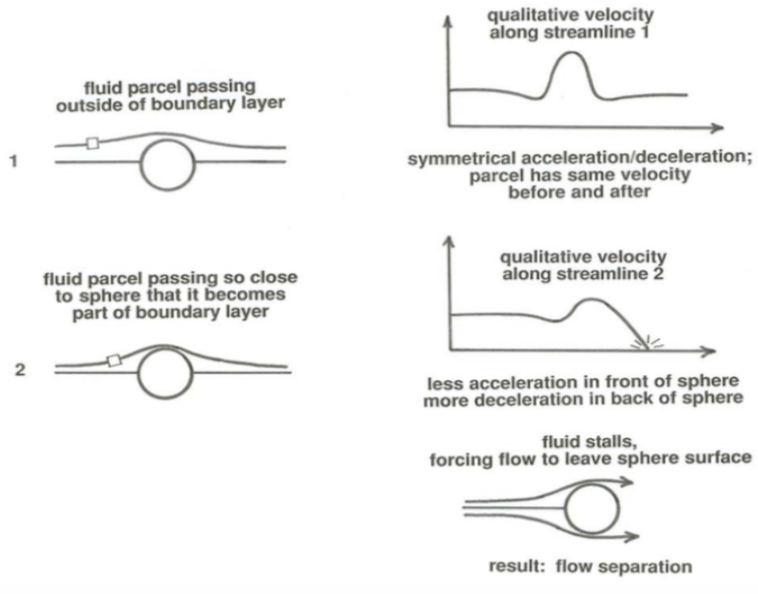

Figure 2.11: Flow processes leading to the onset of flow separation.

Once the separated flow is established, the flow pattern looks something like that shown in (Figure 2.12). This figure is just a detail of the region enclosed by the dashed curves in (Figure 2.8).[10]

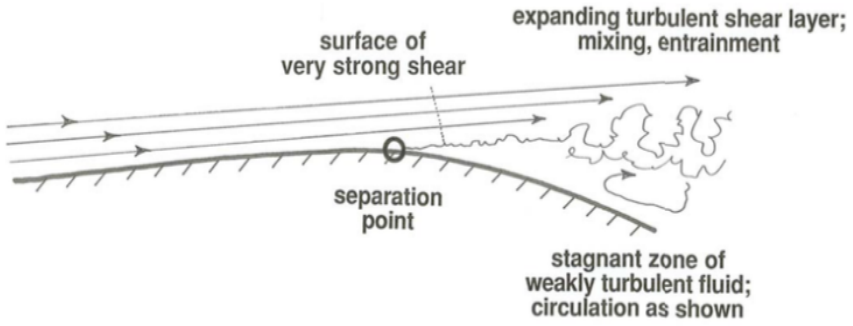

Figure 2.12: Close-up view of flow separation.

2.3.4 Drag Force and Drag Coefficient Concepts

Drag force is an important consideration for engineering designs. Understanding drag and how to decrease it helps people design sturdier structures and bridges that hold up better to wind, more efficient cars and planes, and more efficient collection of wind energy and hydropower.[11]

The drag force always opposes the motion of an object. Unlike simple friction, the drag force is proportional to some function of the velocity of the object in that fluid. This functionality is complicated and depends upon the shape of the object, its size, its velocity, and the fluid it is in. For most large objects such as cyclists, cars, and baseballs not moving too slowly, the magnitude of the Drag Force (FD) is proportional to the square of the speed of the object. We can write this relationship mathematically. When taking into account other factors, this relationship becomes

$$F_{\mathrm{D}} = \frac{1}{2} C \rho A v^2 \tag{2.11}$$

This equation can also be written in a more generalized fashion as

$$F_{\mathrm{D}} = bv^n \tag{2.12}$$

where b is a constant equivalent to 0.5C ρ A.[12]

Drag force is proportional to the velocity for a laminar flow and the squared velocity for a turbulent flow. Drag is generally caused by two phenomena:

- Skin Friction. In general, when a fluid flows over a stationary surface, e.g., the flat plate, the bed of a river, or the pipe wall, the fluid touching the surface is brought to rest by the shear stress at the wall. The boundary layer is the region in which flow adjusts from zero velocity at the wall to a maximum in the mainstream of the flow. Therefore, a moving fluid exerts tangential shear forces on the surface because of the no-slip condition caused by viscous effects. This type of drag force depends especially on the geometry, the roughness of the solid surface, and the type of fluid flow.

- Form Drag. Form drag, also known as pressure drag, arises because of the shape and size of the object. This type of drag force is an interesting consequence the Bernoulli's effect. According to Bernoulli's principle, faster-moving air exerts less pressure, and this causes that there can be a pressure difference between surfaces of the object. The general size and shape of the body are the most important factors in form drag. Generally, bodies with a larger presented geometric cross-section will have higher drag than thinner bodies.

Both of these forces, in general, have components in the direction of flow, and thus the resulting drag force is due to the combined effects of pressure and skin friction forces in the flow direction. When the friction and pressure drag coefficients are available, the total drag coefficient is determined by simply adding them:

$$C_D = C_{D,\text{ friction}} + C_{D,\text{ form}} \tag{2.13}$$

Most drag is due to friction drag at low Reynolds numbers, especially for highly streamlined bodies such as airfoils. On the other hand, the pressure drop is significant at a high Reynolds number, which increases form drag.

The components of the pressure and skin friction forces in the normal direction to flow tend to move the body in that direction, and their sum is called lift.[13]

The drag coefficient is a dimensionless quantity used in drag equation to define the drag or the resistance of an obstacle in a fluid flow, which is generally denoted as Drag Coefficient (CD). A high drag coefficient indicates a significant hydrodynamic or aerodynamic drag on a body. The drag coefficient is a function of the flow velocity, the Re, the flow direction, the object positioning, the object size, the fluid density, and the fluid viscosity Eq (2.13) shows the relationship between the drag coefficient on a particle and the drag force:

$$C_D = \frac{2F_D}{\rho V^2 A} \tag{2.14}$$

where FD is the drag force, ρ is the fluid density, the Velocity (V) of the fluid relative to the particle, and Projected cross-sectional area (A).[11]

2.4 Published results for the Immersed Bodies

The determination of drag coefficients has been the topic of numerous studies (mostly experimental), and there is a huge amount of drag coefficient data in the literature for just about any geometry of practical interest. The drag coefficient, in general, depends on the Reynolds number, especially for Reynolds numbers below about 10^4. At higher Reynolds numbers, the drag coefficients for most geometries remain essentially constant This is due to the flow at high Reynolds numbers becoming fully turbulent. However, this is not the case for rounded bodies such as circular cylinders and spheres The reported drag coefficients are usually applicable only to flows at high Reynolds numbers.[3]

In the case of flow over a sphere, both friction drag and pressure drag contribute to total drag. The drag coefficient for flow over a smooth sphere is shown as a function of Reynolds number

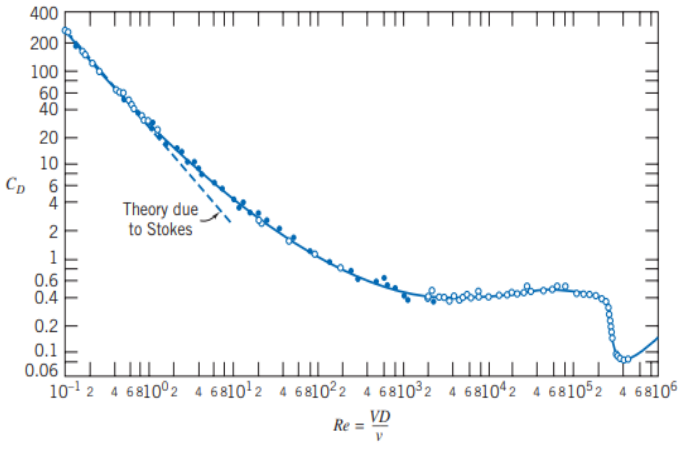

Figure 2.13: Drag coefficient of a smooth sphere as a function of Reynolds number

As the Reynolds number is further increased, the drag coefficient drops continuously up to a Reynolds number of about 1000, but not as rapidly as predicted by Stokes' theory. A turbulent wake (not incorporated in Stokes' theory) develops and grows at the rear of the sphere as the separation point moves from the rear of the sphere toward the front; this wake is at a relatively low pressure, leading to a large pressure drag. By the time Re $\approx$ 1000, about 95% of total drag is due to pressure. For $10^3 < Re < 3 \times 10^5$ the drag coefficient is approximately constant. In this range the entire rear of the sphere has a low-pressure turbulent wake, and most of the drag is caused by the front-rear pressure asymmetry.[14]

At very low Reynolds number, $Re \leq 1$, there is no flow separation from a sphere; the wake is laminar and the drag is predominantly friction drag. Stokes has shown analytically, for very low Reynolds number flows [14] The drag coefficient in this case is inversely proportional to the Reynolds number, and for a sphere it is determined to be

$$C_D = \frac{24}{\mathrm{Re}} \quad (\mathrm{Re} \leq 1) \tag{2.15}$$

Then the drag force acting on a spherical object at low Reynolds numbers becomes

$$F_D = C_D A \frac{\rho V^2}{2} = \frac{24}{\mathrm{Re}} A \frac{\rho V^2}{2} = \frac{24}{\rho V D/\mu} \frac{\pi D^2}{4} \frac{\rho V^2}{2} = 3\pi \mu V D \tag{2.16}$$

which is known as Stokes law, after British mathematician and physicist G. G. Stokes (1819–1903). This relation shows that at very low Reynolds numbers, the drag force acting on spherical objects is proportional to the diameter, the velocity, and the viscosity of the fluid. This relation is often applicable to dust particles in the air and suspended solid particles in water. The drag coefficients for low Reynolds number flows past some other geometries are given in Fig 2.17 . at low Reynolds numbers, the shape of the body does not have a major influence on the drag coefficient.[3]

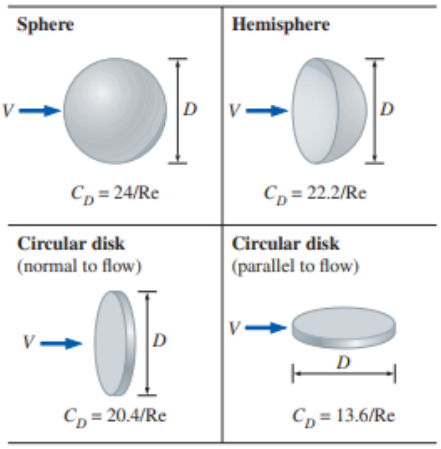

Figure 2.14: Drag coefficients CD at low Reynolds numbers

Roughness affects drag of cylinders and spheres similarly: the critical Reynolds number is reduced by the rough surface, and transition from laminar to turbulent flow in the boundary layers occurs earlier. The drag coefficient is reduced by a factor of about 4 when the boundary layer on the cylinder becomes turbulent[14]

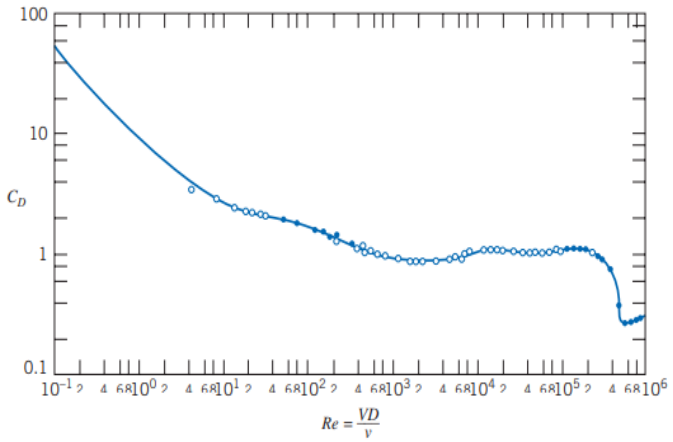

Figure 2.15: Drag coefficient for a smooth circular cylinder as a function of Reynolds number

Cases of two-dimensional and three-dimensional bodies Drag coefficients

The drag coefficients for various two- and three-dimensional bodies are given in (figures 2.17 and 2.18) for large Reynolds numbers. there are several observations from these tables about the drag coefficient at high Reynolds numbers. First of all, the orientation of the body relative to the direction of flow has a major influence on the drag coefficient. For example, the drag coefficient for flow over a hemisphere is 0.4 when the spherical side faces the flow, but it increases threefold to 1.2 when the flat side faces the flow.

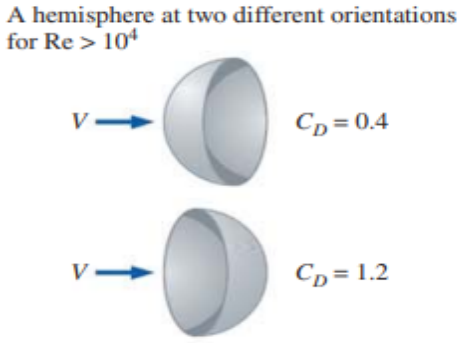

Figure 2.16: Changing a body's orientation (and shape) relative to flow can drastically change its drag coefficient.

For blunt bodies with sharp corners, such as flow over a rectangular block or a flat plate normal to the flow, separation occurs at the edges of the front and back surfaces, with no significant change in the character of flow. Therefore, the drag coefficient of such bodies is nearly independent of the Reynolds number. Note that the drag coefficient of a long rectangular rod is reduced almost by half from 2.2 to 1.2 by rounding the corners.[3]

Representative drag coefficients C_D for various three-dimensional bodies based on the frontal area for Re $> 10^4$ unless stated otherwise (for use in the drag force relation $F_D = C_D A\rho V^2/2$ where V is the upstream velocity)

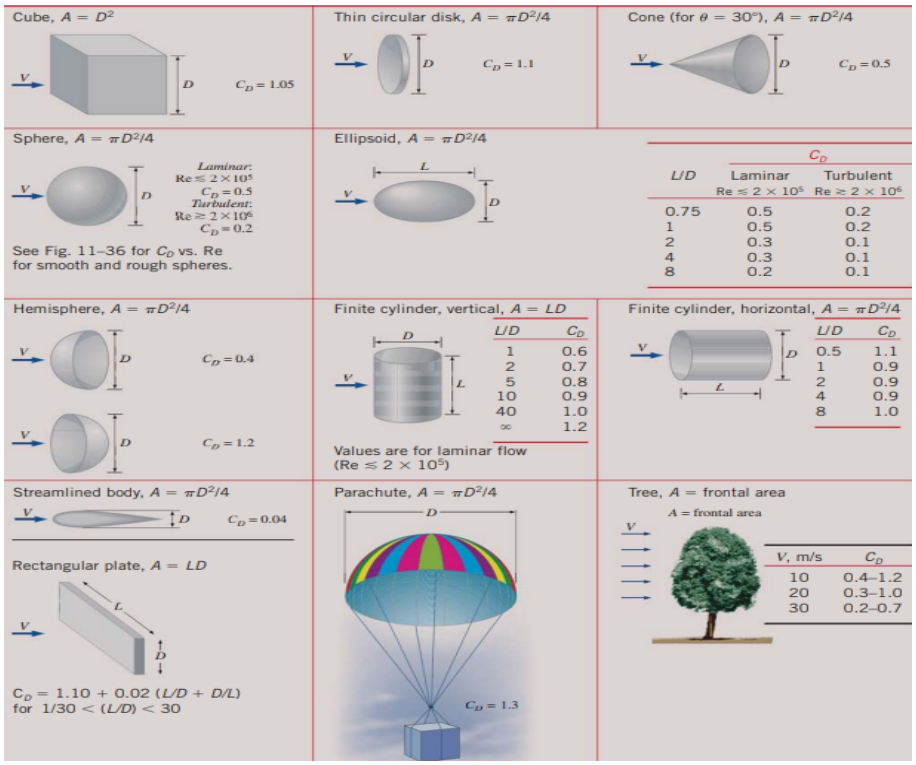

Figure 2.17: three-dimensional

Drag coefficients C_D of various two-dimensional bodies for Re $> 10^4$ based on the frontal area $A = bD$, where b is the length in direction normal to the page (for use in the drag force relation $F_0 = C_0 A\rho V^2/2$ where V is the upstream velocity) [3] Experimental

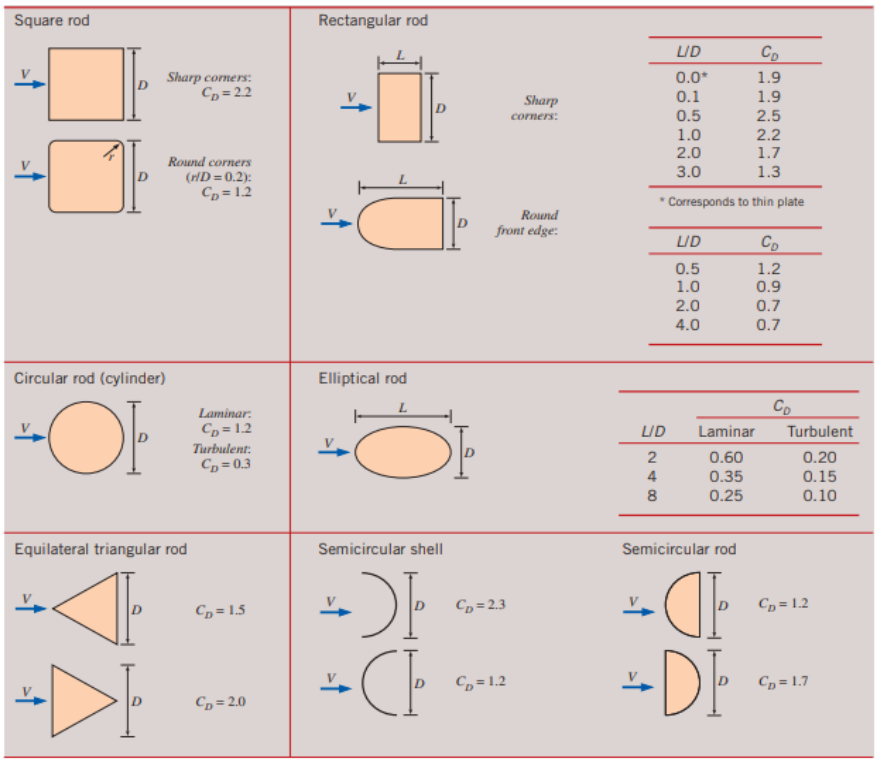

Figure 2.18: two-dimensional bodies

data for drag coefficients on objects must be selected and applied carefully. Due regard must be given to the differences between the actual conditions and the more controlled conditions under which measurements were made.[14]

Chapter 3

Experimental set-up

During this chapter on the experimental setup, we will take a comprehensive look at the hydraulic channel, paying particular attention to its characteristics as well as the various geometries that were selected for the trials.

3.1 Hydraulic channel

Hydraulic channels are utilized to examine and illustrate the characteristics of fluid flow within a regulated setting. These channels generally comprise of transparent walls, a head tank equipped with adjustable gates, a circulating pump, a flow meter, and flow control valves. These simulations are specifically created to replicate authentic hydraulic conditions, enabling the study of different hydraulic structures and fluid meters. An essential component of hydraulic channels is the examination of open-channel flow, which refers to the flow that is not completely confined within inflexible boundaries and has a surface exposed to the atmosphere. The study of open-channel flow heavily relies on the geometric characteristics of channel sections, including parameters such as flow depth, top width, wetted area, and wetted perimeter. The properties mentioned, in addition to the hydraulic radius and hydraulic depth, play a crucial role in determining the characteristics of flow in open channels. An understanding of open-channel flow is crucial in a range of practical contexts, such as the planning and assessment of storm drainage systems,

culverts, and bridges.[15]

Applications of Hydraulic Channels in Industry

Hydraulic channels are utilized in diverse industries for a multitude of purposes. Channels are utilized in various applications, such as agricultural irrigation, navigation for transporting goods, recreational purposes, fluid transfers, facilitating water circulation in hydroelectric power plants for electricity generation, drainage or overflow, and ditches, among others.[15] In the industrial context, hydraulic channels are used for pipe flow, dam design, pumps, turbines, hydropower, computational fluid dynamics, flow measurement, river channel behavior, and erosion[16] They are also crucial in drainage, irrigation, and hydraulic projects, including the design and evaluation of storm drainage systems, culverts, and bridges[17] additionally, hydraulic channels are used in educational settings to help students understand hydraulic principles and their real-world applications.

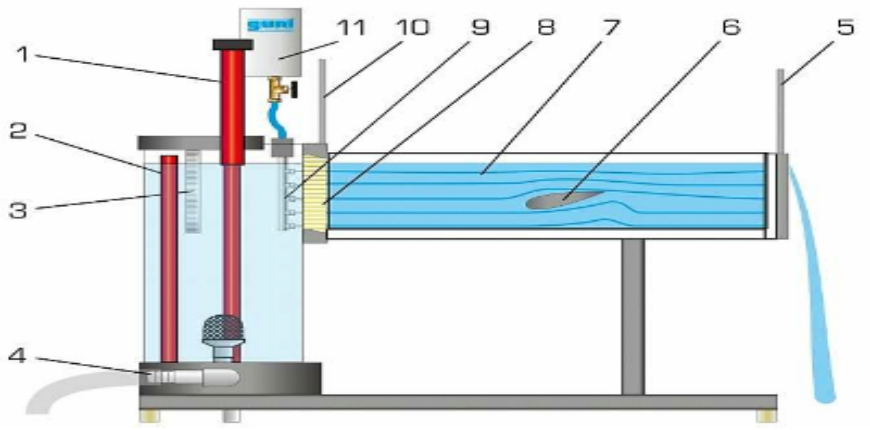

Figure 3.1: Hydraulic Demonstration Channel

1. Adjustable overflow; 2. Tank; 3. Scale; 4. Water supply; 5. Weir at the water outlet; 6. Body; 7. Experimental flume; 8. Flow straightener; 9. Distributor for contrast medium; 10. Sluice gate at the water inlet to the experimental flume; 11 . Tank for contrast medium.[18]

The hydraulic channel was key to the experiments. It is placed in the fluid mechanics laboratory of the Polytechnic Institute of Bragança. The equipment was produced by

Figure 3.2: IPB fluid mechanics lab hydraulic channel.

Engineering Laboratory Design Inc. It has a power rating of 0.56 kW and a channel length of 2.20 meters. Additionally, it possesses a mechanism for controlling the angle.[18]

3.2 Flow Calculation

The procedure for conducting an experimental flow calculation involves narrowing the cross section of the hydraulic channel to accommodate the placement of a duct, which enables the fluid to be directed into an external container.

Figure 3.3: Equipment and methods for experimental flow calculation

The duration between when the duct was inserted into the container and when it was taken out was measured using a timer. However, the outside container did not have a means to measure the capacity. The volume may be established by calculating the difference in mass of the container before and after the fluid is added.

Figure 3.4: Mass of the empty container.

Upon completing the preceding operation, the mass of the container containing the fluid.

Figure 3.5: Mass of container with water.

To calculate the flow rate, you may use the given equation provided you have the specific mass of the water, the difference in mass, and the time taken to fill the container.

$$Q = \frac{m_f - m_0}{\rho \Delta t} \tag{3.1}$$

The following equation is used to determine the fluid velocity inside the region constrained by the acrylic extension:

$$v = \frac{Q}{\pi r_s^2} \tag{3.2}$$

The experimental test parameters are detailed in the table, together with all the values utilized and achieved

Description	**Symbol**	**Valor**
Initial mass of the container	m_O	1,45 kg
Final mass of the container	m_f	30,30 kg
Specific mass of water	ρ	997 kg/m^3
Time measured on the stopwatch	Δt	8,36 s
Flow rate	$\dot{Q}$	0,0034 m^3/s
Section Radius	r_s	0,0375 m
Fluid velocity at the section	v	0,78 m/s

Table 3.1: Parameters of the experimental tests.[18]

Figure 3.6: The configuration of the water tunnel and the slope that defines the velocity.[18]

3.3 Conducted experiments

The experiments were conducted inside the hydraulic channel tunnel. The main goal was to determine the drag coefficient of various geometries in each test. Four simulations were conducted in water density. The process involved placing the submerged body object in a vertical position and exposing it to fluid flow on the opposite side the geometries body was attached with string fishing line where hanging a weight in the beginning of the hydraulic machine to balance the force of the exerted water.

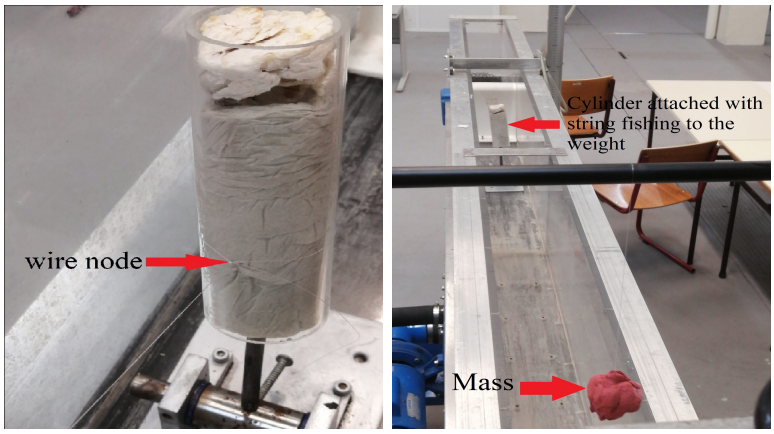

Figure 3.7: Attached weight

Other essential tool were utilized to conduct these experiments. It was crucial to use a customized pivot axis system, which was secured with two screws on both sides, to prevent the geometry from falling forward or backward during the simulation. The system's base was made of a heavy material and fixed with screws on the channel.

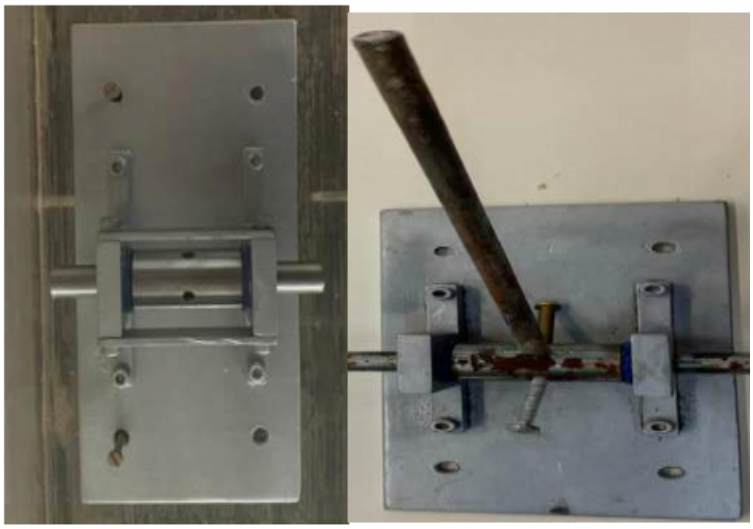

Figure 3.8: Base measurement machine with and without the stick that holds objects.[18]

The objects consisted of two cylinders and two spheres, each with different diameters.

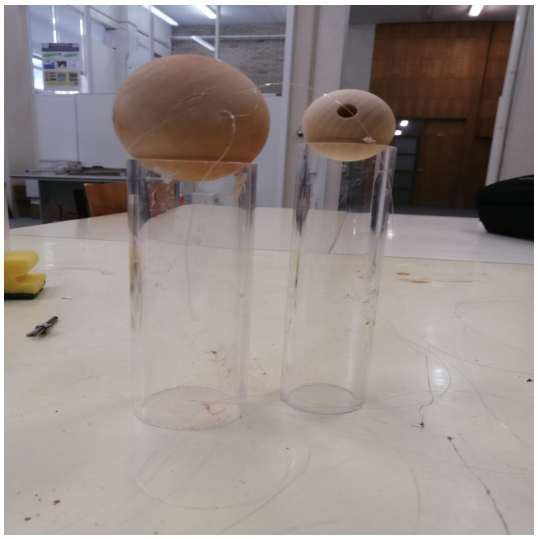

Figure 3.9: Geometries utilized (2 cylinders 2 spheres)

Experiments with geometry 1 (cylinder with 40 mm diameter) – simulation 1

The first simulation made was with the long cylinder ∅40 mm respective diameter and a length of 150 mm. the projected area exposed to the fluid force was A=0.006 m^2, the experiment were performed 5 times on different string positions, in order to determine the center of pressure.

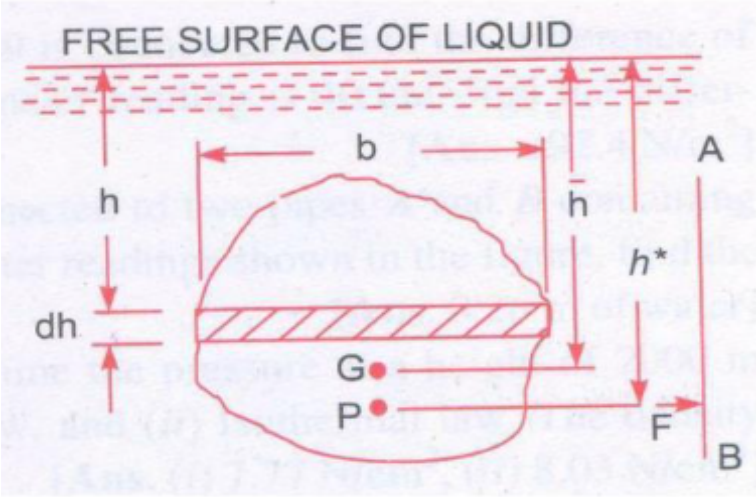

Figure 3.10: Vertical plane surface submerged in liquid.[19]

$$h^* = \frac{I_G}{A\bar{h}} + \bar{h} \tag{3.3}$$

where

$A =$ Total area of the surface

$\bar{h} =$ Distance of C.G. of the area from free surface of liquid

G = Centre of gravity of plane surface

$P =$ Centre of pressure

h* = Distance of centre of pressure from free surface of liquid.

Figure 3.11 displays the five node locations of the long cylinder, together with the corresponding weights at each string position

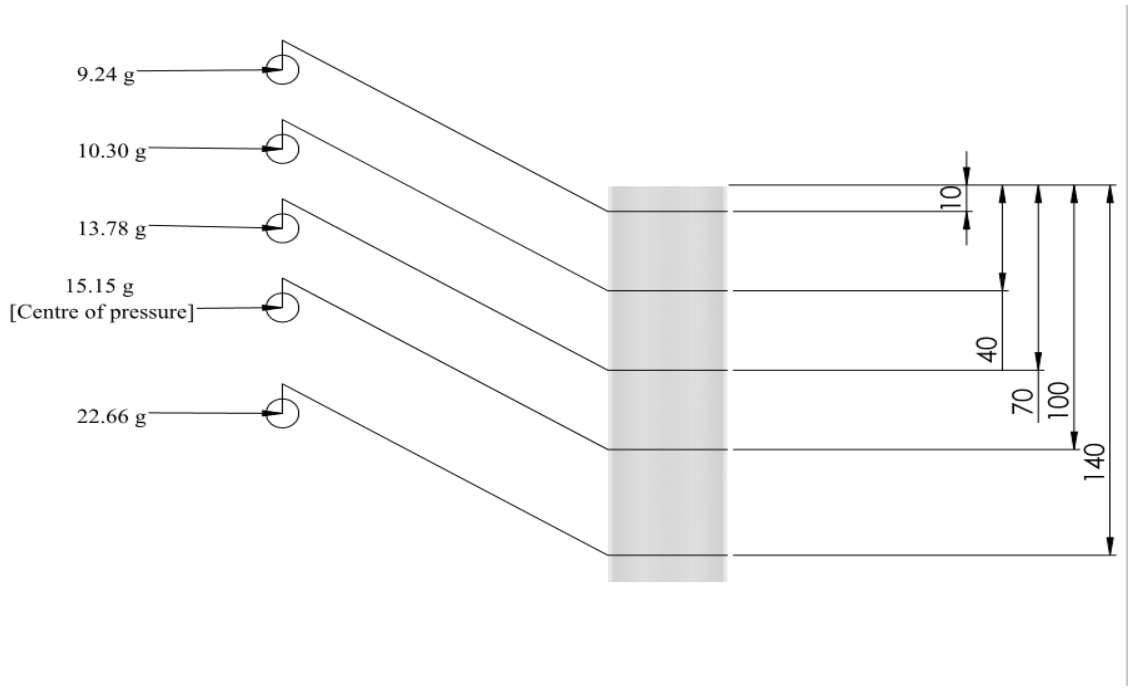

Figure 3.11: String positioning for the long cylinder

Figure 3.12 shows the process of measuring the drag coefficient.

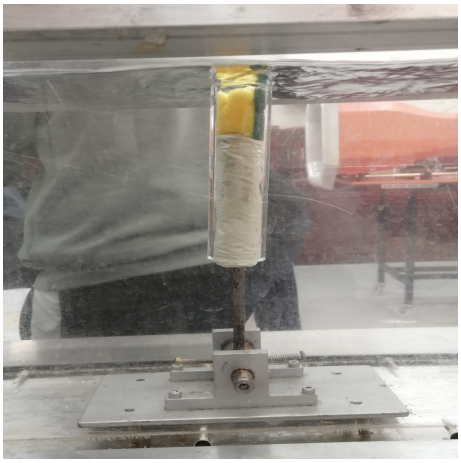

Figure 3.12: Simulation 1 for the long cylinder (string in centre of pressure position)

Once we have achieved a state of balanced equilibrium between the flow velocity and the cylinder, we proceed to measure the weights on the scale for each position of the string

then calculate the drag force where ($F_D = mg$).

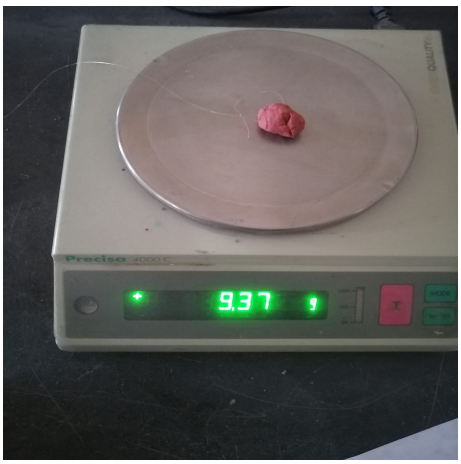

Figure 3.13: Measuring the weight.

Experiments with geometry 2 (cylinder with 50 mm diameter) – simulation 2

the short cylinder ∅50 mm respective diameter and a length of 140 mm. the projected area exposed to the fluid force was A=0.007 m^2, we do replicated the same process as the long cylinder.

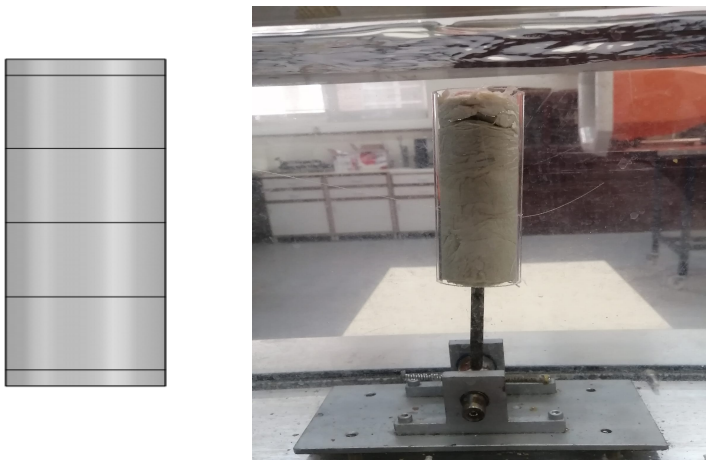

Figure 3.14: Simulation 2 for the short cylinder (string in centre of pressure position)

Experiments with geometry 3 (sphere with 58 mm diameter) – simulation 3

For the third set of experiments was used a sphere with ∅58 mm diameter. The projected area exposed to the flow was A=0,00264074 m^2, and the drag force was measured in the centre of mass of the sphere, attaching the sting to the centre of the sphere.

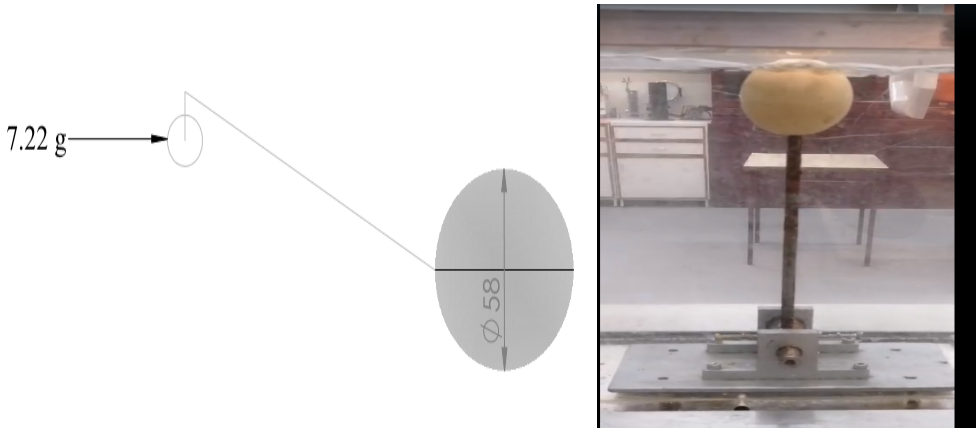

Figure 3.15: The big sphere

Experiments with geometry 4 (sphere with 37 mm diameter) – simulation 4

For the fourth set of experiments was used a small sphere with ∅37 mm diameter. The projected area exposed to the flow was A= 0,00113354 m^2, and the force was also measured at the centre of mass of the sphere.

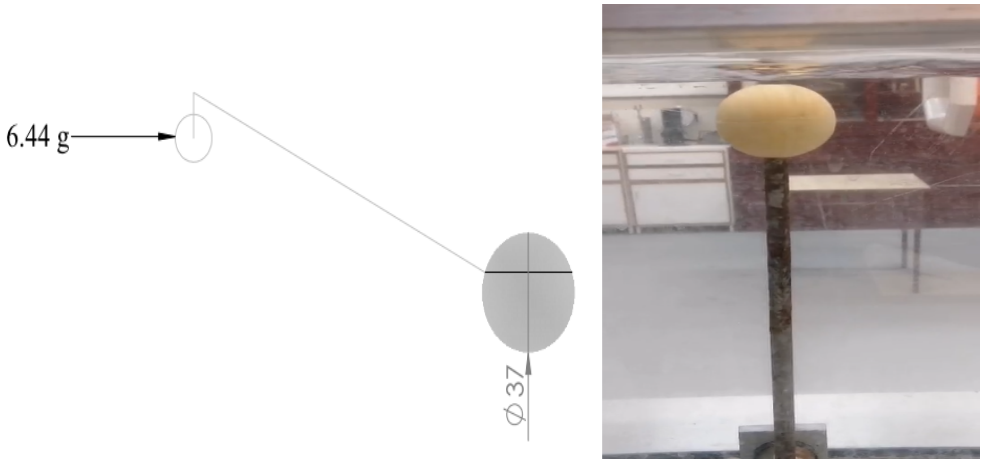

Figure 3.16: The small Sphere

For the 4 simulations, 4 geometries, the experiments were done for two fluids with different viscosities and densities, both Newtonians, first with water and then replicated with a mix of Glycerin and Water. So, in total we carried out 8 sets of experiments, 4 geometries, each with 2 fluids.

Figure 3.17: Glycerin bottle.

To obtain the mix Glycerin-Water 2 liters of glycerin was added to the tank, after the experiments with water, and then measured the viscosity and the density of the mix, taken a sample from the tank. The objective is to possess a fluid viscosity that was differ from water. The dynamic viscosity of the Glycerin-Wat mix was measured using a rheometer that exists in the Lab of Fluid Mechanics.

Chapter 4

Results and Analysis

The main purpose of these experiments is to analyze the drag force coefficients of different geometries immersed in water. This chapter will provide a presentation of the experimental results, which are documented in tables and graphs.

4.1 Experiments Results

We used two geometries, 2 cylinders and 2 spheres, each one with two different dimensions, for a constant velocity of the fluid flow, and for two Newtonian fluid with different viscosities.

Figure 4.1: Geometric shapes employed (2 cylinders 2 spheres)

Geometry	Diameter (mm)	Frontal area (m2)
Cylinder 1	40	0.006
Cylinder 2	50	0.007
Sphere 1	58	0.002641
Sphere 2	38	0.001134

Table 4.1: Objects Measurement and the corresponding Area.

The frontal of the geometry is the area projected in a perpendicular plane to the flow. For the cylinders is a rectangular area (diameter x length) and for the spheres a circular area (πR^2).

The drag force was obtained knowing the mass needed to maintain the geometry in equilibrium, so that the force due to the mass was equal to the drag force (FD = mg).

Consequently, with all the requisite data at hand, it was possible to determine the drag coefficient by equation (2.14).

All experimental results obtained for the 4 geometries, with 2 different fluids are listed in Table 4.2

Geometry	Fluid	Fluid viscosity (mPa.s)	Fluid density (kg/m3)	Re	Mass (g)	Drag Force (N)	Drag Coefficient
Cylinder 1	Water	1	998.2	3394	15.15	0.1486215	6.9
	Water+glycerine	1.1	999	3088	16.94	0.1563714	7.2
Cylinder 2	Water	1	998.2	4242	14.6	0.143226	5.7
	Water+glycerine	1.1	999	3860	14.9	0.146169	5.8
Sphere 1	Water	1	998.2	4921	7.27	0.0713187	7.5
	Water+glycerine	1.1	999	4477	7.39	0.0724959	7.6
Sphere 2	Water	1	998.2	3224	6.44	0.0631764	15.4
	Water+glycerine	1.1	999	2933	6.67	0.0654327	16.0

Table 4.2: Analytical Drag Coefficient

The mass was measured at the center of pressure of the geometries and the Reynolds number calculated by Equation (2.4). The Reynold numbers are always lower than 3×10^5, therefore laminar regime.

4.2 Experimental Analysis

The next graphics show the drag coefficient versus the Reynolds number for all experimental tests.

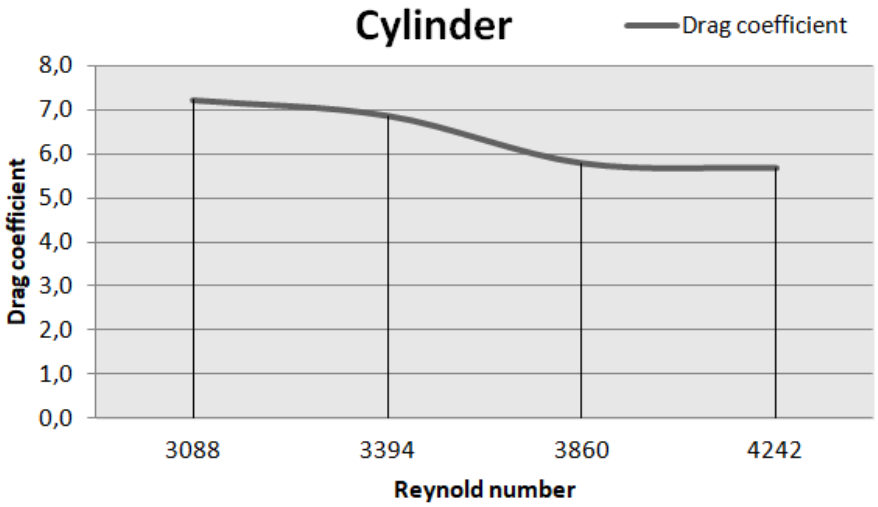

Figure 4.2: Drag Coefficient as a function of reynolds number for cylinder

The Figures 4.2 above shows the drag coefficient with the Reynolds number variation, for both cylinders. As the Reynolds number increases the drag coefficient decreases almost linearly.

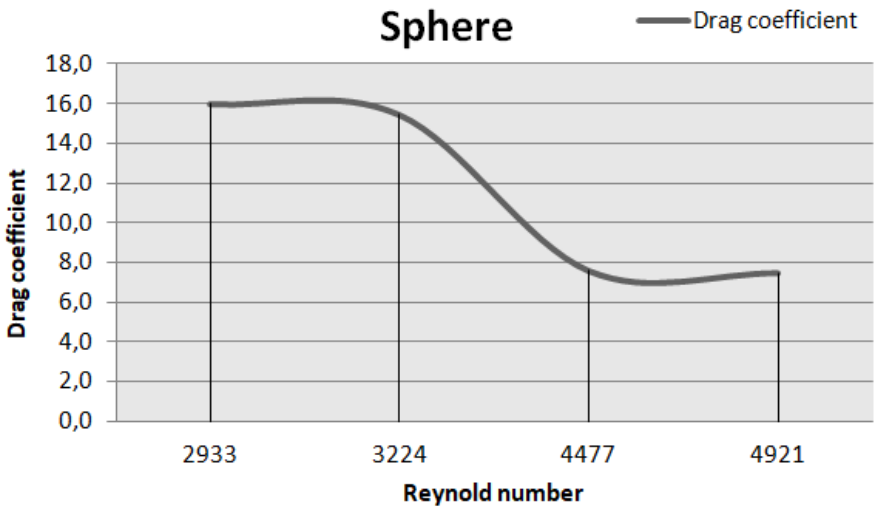

Figure 4.3: Drag Coefficient as a function of Reynolds number for Sphere

As shown above the graphic of Figure 4.3, for the 2 spheres, the drag coefficient also decreases with the Reynolds number, and the flow laminar in all situations.

The same behavior was expected for the Drag Force, as can be seen from the next two Figures.

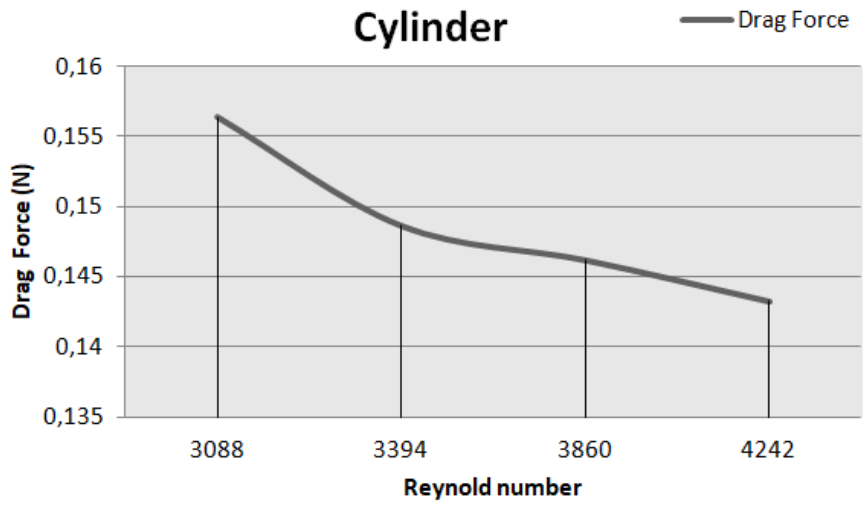

Figure 4.4: Drag Force as a function of the Reynolds number for the cylinder

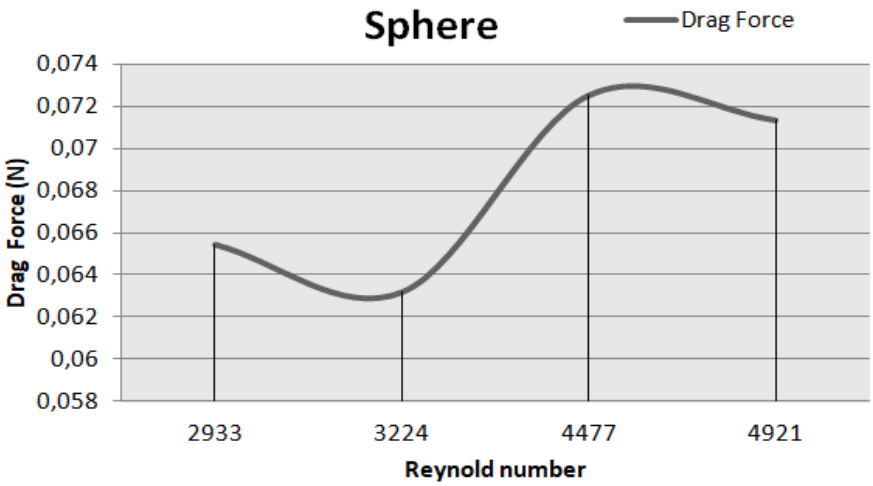

Figure 4.5: Drag Force as a function of the Reynolds number for the spheres

Chapter 5

Conclusions

The 3 main conclusions that we obtain from the experimental results are:

1 – It is well known that viscosity influences the level of resistance (Drag Force) impose by objects in external fluid flows. Fluids with higher viscosity exhibit more resistance, resulting in higher drag forces for objects in motion inside them. In our study the two fluids used in the experiments, water and water/ glycerin, did not provided flows with significant different Reynold numbers, as initially expected because both fluids are Newtonians and practically with the same dynamic viscosity. However, the resistance behavior can been observed from the drag force results in Table 4.2, the higher the fluid viscosity, the higher the drag force.

2- The Figures 4.2 for cylinders, and 4.3 for spheres, show a decrease of the drag coefficient with the increasing Reynolds number, which is consistent with the anticipated results and empirical evidence on the variations in drag coefficient with Reynolds number for cylindrical and spherical objects. Upon comparing the experimental data with the published findings on cylinders and spherical objects, the researches strongly support the acquired results. Figure 2.15 illustrates the drag coefficient for a smooth circular cylinder as it varies with the Reynolds number. It is evident that the plot demonstrates identical behavior within the same range of Reynolds numbers, as seen in Figure 4.2. Additionally, Figure 2.17 depicts three-dimensional entities in the shape of a cylinder and a sphere in the

laminar flow the drag coefficient is higher always than the turbulent flow, and we can observe the impact of the area which is directly proportional to the drag coefficient.

3 – The experiments results allow us to conclude that the experimental setup used, the water channel, is suitable to carry on experiments to obtain drag forces, and so drag coefficients, for different body shapes a different fluids, despite the limitation of the constant velocity, is not possible to vary the velocity fluid flow.

Overall, these experiments provided valuable experimental insights of external flow of cylinders and spheres in different fluid flows conditions. These study highlighted the importance of the precise quantification of the drag force experienced by objects immersed in fluids, improving the understanding of fluid dynamics.

In the future, further research may prioritize the investigation of different body shapes, and primarily for different Reynolds numbers, to cover, if possible, transitional and turbulent flows. Thank might be achieved, in the experimental setup used, with different fluids, different viscosities.

Bibliography

[1] V. B. Aurovinda Mohanty Asst. Prof. Mechanical Engg. Dept, *Fundamentals of Fluid Mechanics*. 2018.

[2] T. E. ToolBox, *Viscosity - absolute (dynamic) vs. kinematic.* https://www.engineeringtoolbox.com/dynamic-absolute-kinematic-viscosity-d_412.html, 2003.

[3] J. M. C. Yunus A. Çengel, *FUNDAMENTALS AND APPLICATIONS, THIRD EDITION*. McGraw-Hill, 2014.

[4] X-engineer, *What is fluid density*, https://x-engineer.org/fluid-density/.

[5] J. P. Johnston, "Internal flows," in *Turbulence*, P. Bradshaw, Ed. Berlin, Heidelberg: Springer Berlin Heidelberg, 1976, pp. 109–169, ISBN: 978-3-662-22568-4. DOI: 10.1007/978-3-662-22568-4_3. [Online]. Available: https://doi.org/10.1007/978-3-662-22568-4_3.

[6] EngineeringClicks, *Reynolds number calculator and formula (equation)*, https://www.engineeringclicks.com/reynolds-number-calculator/, 2017.

[7] F. M. White, *Fluid mechanics*. New York, 1990.

[8] BRUNETTI, *F. Fluid mechanics. 2nd Edition*. São Paulo: Pearson Prentice Hall, 2013.

[9] *What is Reynolds Number (Re)? (Complete Guide) | SimScale*, https://www.simscale.com/docs/simw background/what-is-the-reynolds-number/, Aug. 2023.

[10] J. Southard, *INTRODUCTION TO FLUID MOTIONS AND SEDIMENT TRANSPORT*. CC BY-NC-SA 4.0.

[11] M. Yuce and D. Kareem, "A numerical analysis of fluid flow around circular and square cylinders," *Journal - American Water Works Association*, vol. 108, E546–E554, Oct. 2016. DOI: 10.5942/jawwa.2016.108.0141.

[12] J. S. William Moebs Samuel J. Ling, *University physics volume 1*, https://openstax.org/books/university-physics-volume-1/pages/1-introduction, Sep. 2016.

[13] Nuclear-Engineering, *What is drag – air and fluid resistance*, https://www.nuclear-power.com/nuclear-engineering/fluid-dynamics/what-is-drag-air-and-fluid-resistance/, 2016.

[14] J. C. L. PHILIP J. PRITCHARD, *Fox and McDonald's INTRODUCTION TO FLUID MECHANICS EIGHTH EDITION*. JOHN WILEY SONS, INC., 2011.

[15] edibon, *Hydraulic channel machine*, https://www.edibon.com/en/fluid-mechanics/hydraulic-channels.

[16] dantecdynamics, *Hydraulics hydrodynamics*, https://www.dantecdynamics.com/applications/hydraulics-hydrodynamics/.

[17] M. C. simulation engineering team, *Hydraulic structures in civil engineering*, https://www.mr-cfd.com/industries/hydraulic-structures-engineering/.

[18] S. Echi, *Drag coefficients in hydraulic channel*. Escola Supeior de Tecnologia e Gestão of the Instituto Politécnico de Bragança, 2021.

[19] E. E. Al.Swaity, *Hydrostatic Forces on Surfaces*. University of Palestine College of Engineering Urban Planning Applied Civil Engineering, Sep 17, 2014.